Modelling the backscatter from spherical cavities in a solid matrix: Can an effective medium layer model mimic the scattering response?

2011 J. Phys.: Conf. Ser. 269 012016

(http://iopscience.iop.org/1742-6596/269/1/012016)

Journal of Physics: Conference Series **269** (2011) 012016 doi:10.1088/1742-6596/269/1/012016

Modelling the backscatter from spherical cavities in a solid matrix: can an effective medium layer model mimic the scattering response?

Valerie J. Pinfield and Richard E. Challis

Electrical Systems and Applied Optics Division, Faculty of Engineering, University of Nottingham, University Park, Nottingham NG7 2RD

valerie.pinfield@nottingham.ac.uk

Abstract. Industrial applications are increasingly turning to modern composite layered materials to satisfy strength requirements whilst reducing component weight. An important group of such materials are fibre/resin composites in which long fibres are laid down in layers in a resin matrix. Whilst delamination flaws, where layers separate from each other, are detectable using traditional ultrasonic techniques, the presence of porosity in any particular layer is harder to detect. The reflected signal from a layered material can already be modelled successfully by using the acoustic impedance of the layers and summing reflections from layer boundaries. However, it is not yet known how to incorporate porosity into such a model. The aim of the work reported here was to model the backscatter from randomly distributed spherical cavities within one layer, and to establish whether an effective medium, with a derived acoustic impedance, could reproduce the characteristics of that scattering. Since effective medium models are much more readily implemented in simulations of multi-layer structures than scattering per se, it was felt desirable to simplify the scattering response into an effective medium representation.

A model was constructed in which spherical cavities were placed randomly in a solid continuous matrix and the system backscattering response was calculated. The scattering from the cavities was determined by using the Rayleigh partial-wave method, and taking the received signal at the transducer to be equivalent to the far field limit. It was concluded that even at relatively low porosity levels, the received signal was still "layer-like" and an effective medium model was a good approximation for the scattering behaviour.

1. Introduction

Industrial applications are increasingly turning to modern composite layered materials to satisfy strength requirements whilst reducing component weight. An important group of such materials are fibre/resin composites in which long fibres are laid down in layers in a resin matrix. Amongst the significant faults which need to be detected by inspection methods, are delamination flaws, which can be detected by standard ultrasonic techniques, and porosity, which cannot. Currently, models can be used to simulate the reflected signal from a typical multi-layer composite system by summing the reflections from each interface using estimates for the acoustic impedance of each layer. However, it is not yet fully understood how to incorporate porosity into such a multi-layer model. A number of workers have investigated the problem by using modified elastic properties [1-2], for the mixed fibre/resin/porosity composite whilst others have considered the frequency-dependent attenuation

resulting from the cavities [3-4]. Multi-layer models which incorporate porosity through such property mixture-rules and porosity-induced attenuation have been recently reported [5]. Other workers have considered the porous layer as an equivalent homogeneous medium having effective properties derived from the ensemble-averaged reflection and transmission responses [6-10].

However, since a real sample has fixed locations for the cavities, any measurement made during inspection is not an ensemble-averaged response, but the actual scattered signal from cavities at specific locations. The aim of the current work was to investigate the conditions under which an ensemble-averaged or effective-medium description of the material is a good approximation for the signal received from distributed cavities in a single snapshot measurement. We are exploring the emergence of the effective-medium behavior, rather than studying the emerged behavior itself. The question was addressed by formulating a model for the backscattered signal from distributed porosity, and comparing with a simple impedance-based effective-medium model. Whilst our longer-term aim is to establish properties for porous fibre/resin composite, the work reported here investigates the properties of a material which has porosity in a homogeneous matrix. Scattering from fibres themselves will be considered at a later stage.

The two models are presented in the next section: one an "effective-medium" model which treats the reflections from the layer interfaces using the acoustic impedance of the material, and the second a scattering model which considers the signal scattered by individual cavities in the layer. Results from each model are shown and compared in section 4. and final conclusions are summarized in section 5.

2. Scattering from a Single Spherical Cavity

Before considering the system as a whole, it is first necessary to establish the scattering characteristics of the individual pores, which are modelled as spheres of vacuum for simplicity. The Rayleigh partial-wave method can be used to determine the scattering coefficients for a single spherical cavity in a solid medium using a planar incident wave [11] which in the notation of later workers (see Challis et al. [12] for definitions) can be written in the limit of low frequency as

$$A_0 \approx \frac{2}{3} i \left(ka\right)^3 \quad A_1 = -\frac{1}{9} i \left(ka\right)^3 \quad A_2 \approx \frac{1}{24} i \left(ka\right)^3 \tag{1}$$

These results assume a ratio of shear to longitudinal wave speeds of 0.5 as found in many materials; within this assumption the coefficients at low frequency depend only on the wavenumber of the medium, k and the radius of the cavity, a, and not on other physical properties of the medium. In the model, the scattering coefficients are calculated numerically from the boundary condition matrix equation which extends the validity up to ka~0.8; these analytical results, valid at low frequency, permit the frequency and radius dependence to be identified.

The displacement potential of the scattered longitudinal wave in a solid material in the far-field is

$$\varphi \to f\left(\theta,\phi\right)\frac{e^{ikr}}{r} \text{ as } r \to \infty \tag{2}$$

with $f\left(\theta,\varphi\right)$ the scattering amplitude, given in the forward and backward directions respectively by

$$f_0 = \frac{1}{ik}\sum_{n=0}^{\infty}\left(2n+1\right)A_n \approx \frac{13}{24}k^2a^3, \qquad f_\pi = \frac{1}{ik}\sum_{n=0}^{\infty}\left(2n+1\right)A_n\left(-1\right)^n \approx \frac{29}{24}k^2a^3 \tag{3}$$

Hence, both forward and backward scattered amplitudes are dependent on the square of frequency and the cube of cavity radius at low frequency. A time-dependence of $e^{-i\omega t}$ has been assumed throughout.

3. The Two Models

The system configurations for the two models are shown in Figure 1. In both cases, only a single region of modified material is considered for simplicity – that is the space between z_{min} and z_{max} from the transducer face. The solid material of layers 1 and 3 and the matrix surrounding the cavities have

the same acoustic impedance and density as a 70% carbon fibre-resin composite material. The transducer is directly coupled to the solid material.

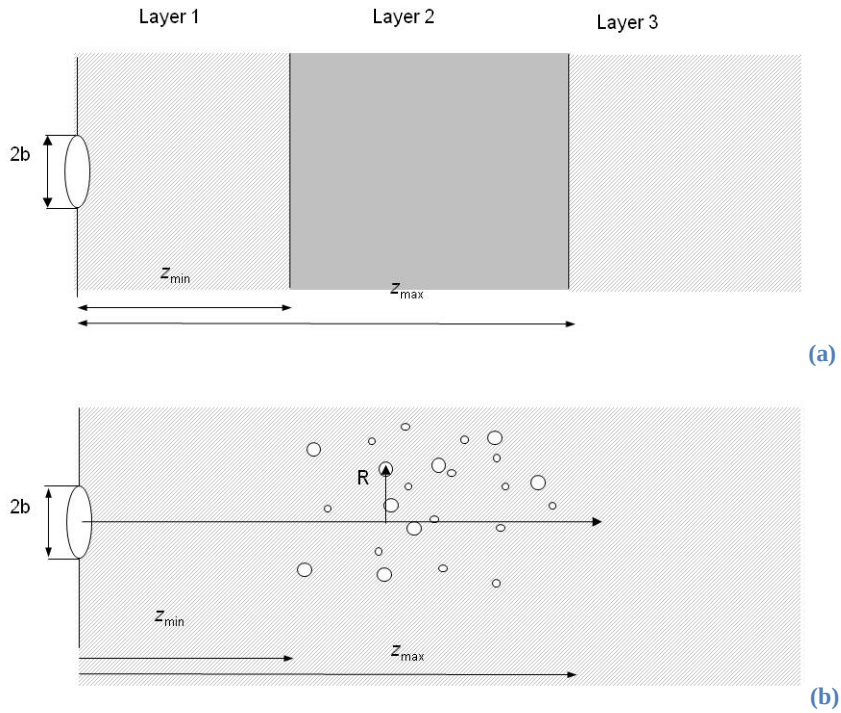

Figure 1 Configuration of the effective medium (a) and discrete scatterer (b) models.

3.1. Effective medium model

Following other workers, the porous layer is treated as a homogeneous material with effective properties, which determine the reflection and transmission responses of the layer [7-8]. For the effective medium model (Figure 1a), layer 2 represents a fibre/resin composite layer with porosity, and layers 1 and 3 non-porous composite material with density, ρ and sound speed, c. Each material is defined by its acoustic impedance, and the signal received at the transducer is obtained by summing the reflections from the front and back interfaces of layer 2. The density of layer 2 can be obtained from the cavity volume fraction, ϕ, thus $\rho_2 = \rho(1-\phi)$. The sound speed in the porous layer, c_2, can be estimated using the effective wavenumber for a medium of randomly distributed scatterers. We have used the single-scattering approximation derived by Foldy [13] extended to non-isotropic scatterers, later confirmed by the multiple-scattering models of workers such as Lloyd and Berry [14]. Thus, the wavespeed can be estimated from the equation

$$\frac{c^2}{c_2^2} \approx 1 + \frac{3\varphi}{k^2 a^3} \mathrm{Re}\, f(0) \approx 1 + 3 \cdot \frac{13}{24}\varphi \qquad (4)$$

using the scattering amplitude of the cavities (1) at the very low frequency limit (*ka*~0.2) to illustrate the frequency dependence. In the model, the calculations are carried out with the full boundary matrix solution, so are valid over a wider range up to around *ka*~0.8. Unsubscripted quantities refer to the non-porous composite. The sound speed in the low frequency, long wavelength limit (wavelength much longer than the cavity radius) is approximately independent of frequency, despite the strong frequency-dependence of the scattering amplitude. Thus the acoustic impedance of the porous layer $Z_2 = \rho_2 c_2$, is also frequency-independent at low frequency, and less than the impedance of the non-porous material. Other studies which have adopted an effective acoustic impedance to model the

response of a layer of scatterers have extended the definition by using the form $Z = \rho\omega/k$ [15-16]. We can express the ratio of the acoustic impedance in the porous and non-porous composite as $\hat{Z} = Z_2/Z$. The signal received at the transducer is the sum of reflections from the interfaces and can be readily expressed as a system frequency response [17]

$$F_{\text{eff}}(\omega) = F_0(\omega)H(\omega) \tag{5}$$

where $F_0(\omega)$ is the frequency-domain transducer response and

$$H(\omega) = e^{2(i\omega/c-\alpha)z_{\min}} \cdot r_{12}\left[1 - t_{12}t_{21}e^{2(i\omega/c-\alpha)d}R(\omega)\right] \tag{6}$$

where the wavenumber $k = \omega/c + i\alpha$ with attenuation α; t_{12} and t_{21} are the pressure transmission coefficients in each direction at the boundary between layers 1 and 2, and r_{12} is the pressure reflection coefficient at that boundary for waves emanating from the transducer, given by

$$r_{12} = \left(\hat{Z}-1\right)\Big/\left(\hat{Z}+1\right), \quad t_{12} = 2\hat{Z}\Big/\left(\hat{Z}+1\right) \text{and } t_{21} = 2\Big/\left(\hat{Z}+1\right) \tag{7}$$

The multiple reflection term sums to $R(\omega) = \left[1 - r_{12}^2\, e^{2(i\omega/c-\alpha)d}\right]^{-1}$ and $d = z_{\max} - z_{\min}$ is the thickness of the layer. We now have a model for the signal received at the transducer from a single layer which has different properties from those around it. We have derived acoustic impedance for a porous layer based on its sound speed and density, but using the layer reflection model any impedance can be supplied for layer 2. By comparing the reflection response with that of the discrete model we will derive the acoustic impedance of the material. Scattering from individual cavities is not included in this model, and diffraction due to finite transducer size has been neglected in both models.

3.2. Discrete scatterer model

Whereas the effective medium model treats only the reflections of a plane wave from the interfaces between regions of different properties, the discrete scatterer model considers each cavity as a secondary source of spherical sound waves which can be detected at the transducer. As shown in Figure 1b, the discrete scatterer model simulates the scattering by spherical cavities located in the region $z_{\min}$ to $z_{\max}$ from the transducer. There are no planar interfaces between materials of different types in this model: the fibre-resin composite (taken as homogeneous) modeled in regions 1 and 3 of the effective medium configuration (Figure 1a) is the same as the matrix surrounding the cavities in the scatterer model. Scatterers are placed randomly in the specified region (overlap is ignored), within the transducer cylindrical "beam" volume, and the incident wave at each scatterer is assumed to be planar. Only single-scattering is modeled.

The signal received at the transducer is taken to be the sum of the far-field scattered waves produced by each of the cavities. For a single scatterer, located at a distance z_j from the transducer, the far-field frequency-domain signal received at the transducer is given by

$$F(\omega) = F_0(\omega)\frac{f_\pi}{z_j}e^{-2\alpha z_j}e^{2i\omega z_j/c} \tag{8}$$

For a number of scatterers, N_{Sc}, distributed in the space, the received signal can be obtained by summation

$$F(\omega) = F_0(\omega)\sum_{j=1}^{N_{Sc}}\frac{f_\pi}{z_j}e^{-2\alpha z_j}e^{2i\omega z_j/c} \tag{9}$$

The simulation predicts the signal received from a single configuration of discrete scatterer locations. As such it represents a typical measurement in a real sample, in which the locations of the cavities are fixed, in contrast to an ensemble-averaged model which is by definition an average over all possible scatterer locations.

3.3. System Properties

The properties for the modelled systems are given in Table 1. The fibre/resin composite material is taken to be a homogeneous solid, with physical properties similar to that of a 70% fibre-resin composite mixture, derived from previous models [18]. The longitudinal sound speed was 3035 ms^{-1}, shear wave speed 1517 ms^{-1} and density 1564 kgm^{-3}. The attenuation of the composite was taken to be zero for the calculations, in order to investigate the effects of scattering only, in the absence of attenuation effects. Scattering from the fibres themselves will be addressed in a later study. A small radius transducer was chosen in order to minimize the effects of diffraction which were considered in an additional study. The transducer response was obtained experimentally using a pair of 10 MHz centre-frequency transducers in water and the signal was sampled using an oscilloscope and then sub-sampled to the required sampling frequency of 50MHz. This process gave an experimentally valid signal with which to perform the calculations. The long wavelength approximation is only valid up to a frequency of ~10MHz for the pore size used in the calculations; however, the full solution for the scattering coefficients (valid at any *ka*) and sound speed was used in the calculations at all frequencies. Only the analytical solutions to the scattering coefficients assume a low frequency limit; all other parts of the model are valid at any frequency range. Calculations were carried out using MATLAB [19].

Distance z_{min}	10 mm	Transducer centre frequency	10 MHz
Layer thickness	1.2 mm	Sampling frequency	50 MHz
Transducer radius	1 mm	Number of samples in signal	1024
Cavity radius	10 μm		

Table 1 Properties of the systems modelled.

4. Results

Calculations were carried out to model the signal received at the transducer according to the two models: the effective medium model and the discrete scatterer model. The time-domain signal predicted by the effective medium model is shown in Figure 2, alongside the transducer signal. All signals have been time-shifted so that the zero occurs at the first signal expected to be received from the front interface of layer 2. The received signal predicted by the effective medium model includes a reflection from the front interface of the layer, and a second reflection from the back interface, with the appropriate time-delay. A comparison with the transducer signal shows that the effective medium model predicts that the signal is inverted at the front interface, but not at the back interface, due to the lower acoustic impedance in the layer compared with the material around it. The shape of the waveform is almost identical to the transducer signal, consistent with the flat frequency response in the effective medium model.

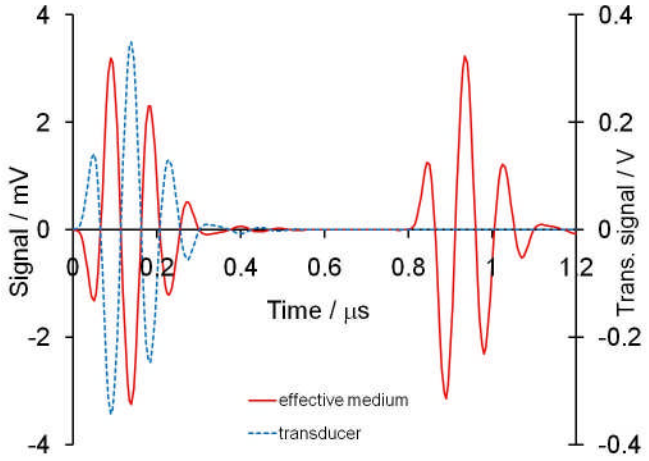

Figure 2 Time-domain signal from the effective medium model (red, solid line) compared with the transducer signal (blue, dashed line). Signals are time-shifted by the propagation time from transducer to the front interface and back.

To investigate the results of the discrete scatterer model, we first observe the signal received from a single isolated cavity embedded in the composite matrix (Figure 3). The shape of the waveform is somewhat modified, due to the frequency-dependence of the scattering amplitude (see section 2.), but the signal is largely in-phase with the transducer signal. This is consistent with the analytical result (8), with f_π real and positive.

Next we consider the signal received when there are a number of cavities located in the defined region. The predicted signals, given by (9), are shown in Figure 4a-c, scaled by volume fraction in order to permit plotting of all results on the same axes. Each plot is the result of a single configuration of the scatterer positions. At the lowest volume fraction (1%) there is a significant scattered signal for the whole duration of the time-window, as the transducer receives scattered sound waves from each individual cavity placed anywhere in the region. However, there is a stronger signal corresponding to the times at which a front-face and back-face reflection would appear. Destructive interference between scattered waves from nearby cavities in the middle of the region results in a stronger signal corresponding to the front and back-face reflections. As the concentration of cavities is increased, the interference effect becomes stronger, and the apparent "front- and back-face" signals are more clearly demarked from the much smaller signal in the intervening period. At the highest concentration, the signal looks very much like that expected from a homogeneous layer in the same region.

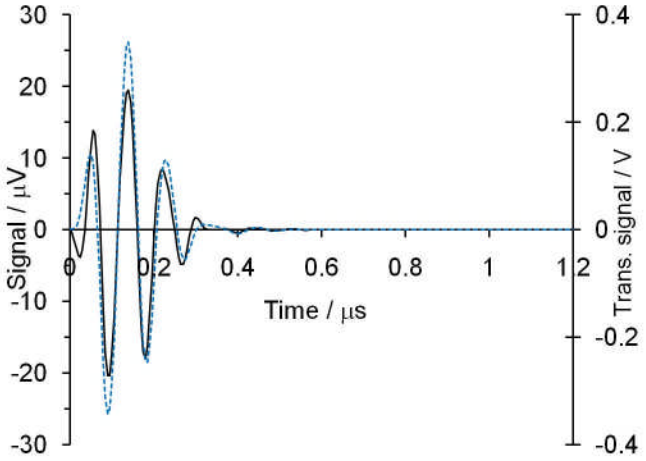

Figure 3 Time-domain signal received from a single spherical cavity (black, solid line) located at a distance of 10mm from the transducer, time-shifted to remove the time-delay, compared with the transducer signal (blue, dashed line).

A measure of the layer-like nature of the signal can be obtained by calculating the ratio of the largest peak height in middle region to the largest peak height in the first group. In Figure 5 this parameter is plotted as a function of concentration, clearly showing that even at 1% porosity the middle interference region is significantly smaller than the apparent "front-interface" reflection. It should be noted, that there are no interfaces between different materials in this model, only cavities in an otherwise homogeneous medium. The response has similarities to reflections from interfaces due to destructive interference between signals scattered by individual cavities within the body of the porous layer.

Here we have demonstrated a typical signal which would be seen from a measurement of a real system i.e. a single configuration of scatterer (cavity) positions. Increasing the number of scatterers in the discrete scatterer model leads to a system response which is closer to an effective medium response, with apparent layer boundary reflections. Thus, as the number density of cavities increases, the system response becomes akin to an expected ensemble-averaged response. Although at 20% porosity, multiple scattering effects are likely to become significant, the results of the single-scattering model are presented to illustrate the tendency towards homogeneous layer characteristics at higher

concentrations. Our results illustrate the degree of appropriateness of applying effective, ensemble-averaged properties at various concentrations. For the small, spherical cavities studied here, a composite containing even a relatively low concentration (1-2%) of cavities could feasibly be treated as an effective medium as long as they are randomly distributed. Only a single snapshot of scatterer positions has been studied, as would be observed in an experimental measurement on a real composite, but clear trends towards effective medium characteristics have been observed. These effects are explored further in a later paper. Although effective-medium behavior does emerge from the discrete-scatterer model, there are differences between the emerging response and the effective medium model. These will be investigated in a later paper, but in summary a difference in both phase shift and frequency response has been identified between the simple effective medium chosen here, and the discrete scatterer model.

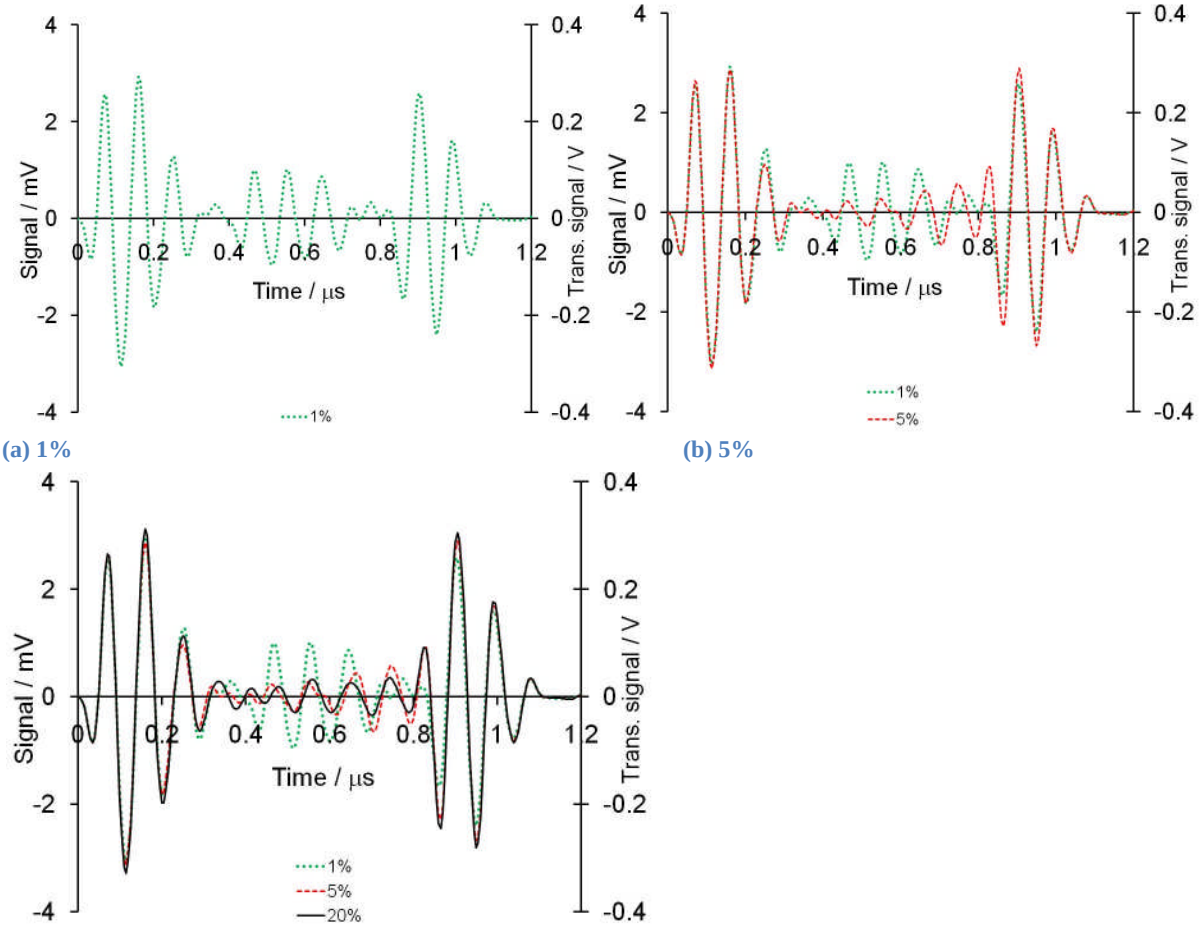

(a) 1% (b) 5%

(c) 20%

Figure 4 Time-domain signal received from randomly distributed spherical cavities at various volume fractions, scaled by volume fraction and time-shifted (a) 1% (b) 5% (c) 20% (earlier results greyed out for comparison).

5. Conclusions

The aim of the work was to establish whether a simple "layer" model would be able to reproduce the characteristics of scattering from cavities in fibre/resin composites. We have established that

- the backscattered signal from randomly distributed spherical cavities does have strong similarities to the signal reflected by a layer, including an apparent "front-" and "back-interface" reflection.
- as the number of scatterers (cavities) is increased, the system response becomes closer to that of an effective medium model.
- the simple effective medium model reproduced many of the features of the discrete scatterer model, but with some differences in the time domain, and in the frequency domain response.

Hence, we conclude that an acoustic-impedance-based multi-layer model will be able to incorporate the effects of porosity (even at relatively low concentrations) in fibre/resin composite materials by use of modified effective properties in an effective-medium model. Further study of the time and frequency domain response is in progress and will be presented in a future publication. It is anticipated that this development will improve techniques for porosity detection in such materials.

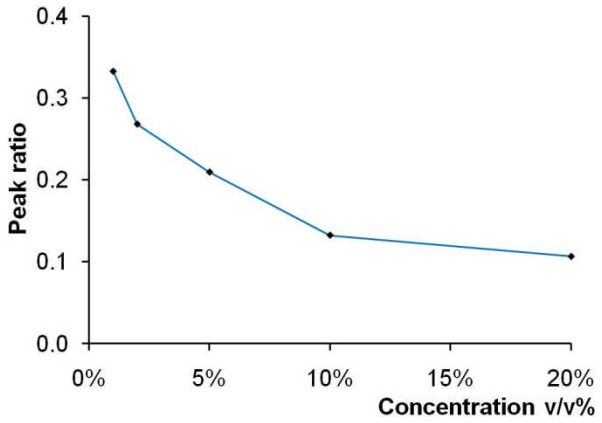

Figure 5 The ratio of the largest peak in the middle region to the largest peak in the first group as a function of concentration. Each point is from a single realisation of scatterer positions.

6. Acknowledgements

Thanks are due to Dr. Andrew Holmes and Mr. Robert Smith (QinetiQ Ltd., Farnborough, UK) for helpful discussions.

References

[1] Martin B G 1977 Ultrasonic attenuation due to voids in fibre-reinforced solids containing voids. *Journal of applied physics* **48** 3368-73
[2] Greszczuk L B 1971 Interfilamentary stresses in Filamentary Composites *American Institute of Aeronautics and Astronautics Journal* **9** 1274-80
[3] Nair S M, Hsu D K and Rose J H 1989 Porosity estimation using the frequency dependency of the ultrasonic attenuation *Journal of nondestructive evaluation* **8** 13-26
[4] Adler L, Rose J H and Mobley C 1986 Ultrasonic Method to Determine Gas Porosity in Aluminum-Alloy Castings - Theory and Experiment *Journal of Applied Physics* **59** 336-47
[5] Mienczakowski M J, Holmes A K and Challis R E 2008 *Review of Progress in Quantitative Nondestructive Evaluation, Vol 27a and 27b,* ed D O Thompson and D E Chimenti pp 995-1001
[6] Parnell W J, Abrahams I D and Brazier-Smith P R 2010 Effective properties of a composite half-space: exploring the relationship between homogenization and multiple scattering theories *Quarterly Journal of Mechanics and Applied Mathematics* **63** 1-32
[7] Angel Y C and Aristegui C 2005 Analysis of sound propagation in a fluid through a screen of scatterers *J. Acoust. Soc. Am.* **118** 72-82
[8] Robert S and Conoir J M 2007 Reflection and transmission process from a slab-like region containing a random distribution of cylindrical scatterers in an elastic matrix *Acta Acustica United with Acustica* **93** 1-12
[9] Aristegui C and Angel Y C 2002 New results for isotropic point scatterers: Foldy revisited *Wave Motion* **36** 383-99
[10] Le Bas P Y, Luppe F and Conoir J M 2005 Reflection and transmission by randomly spaced elastic cylinders in a fluid slab-like region *J. Acoust. Soc. Am.* **117** 1088-97

[11] Ying C F and Truell R 1956 Scattering of a plane longitudinal wave by a spherical obstacle in an isotropically elastic solid *Journal of applied physics* **27** 1086-97
[12] Challis R E, Povey M J W, Mather M L and Holmes A K 2005 Ultrasound techniques for characterizing colloidal dispersions *Rep. Prog. Phys.* **68** 1541-637
[13] Foldy L L 1945 The multiple scattering of waves *Physical review* **67** 107-19
[14] Lloyd P and Berry M V 1967 Wave propagation through an assembly of spheres IV Relations between different multiple scattering theories *Proceedings of the physical society, London* **91** 678-88
[15] Aristegui C and Angel Y C 2007 Effective mass density and stiffness derived from P-wave multiple scattering *Wave Motion* **44** 153-64
[16] Conoir J M, Robert S, El Mouhtadi A and Luppe F 2009 Reflection and transmission at low concentration by a depth-varying random distribution of cylinders in a fluid slab-like region *Wave Motion* **46** 522-38
[17] Challis R E, Freemantle R J, White J D H and Wilkinson G P 1995 Ultrasonic compression wave NDT of adhered metal lap joints of uncertain dimensions *INSIGHT* **37** 954-63
[18] Mienczakowski, M. 2010. Thesis submitted for PhD, University of Nottingham
[19] MATLAB® version R2008a (v. 7.6.0.324), The Mathworks Inc., Natick, U.S.A.